J Geod (2010) 84:19–30
DOI 10.1007/s00190-009-0341-2

ORIGINAL ARTICLE

Atmospheric and oceanic forcing of the rapid polar motion

Christian Bizouard · L. Seoane

Received: 13 March 2009 / Accepted: 18 August 2009 / Published online: 3 September 2009

Abstract The rapid polar motion for periods below 20 days is revisited in light of the most recent and accurate geodetic and geophysical data. Although its amplitude is smaller than 2 mas, it is excited mostly by powerful atmospheric processes, as large as the seasonal ones. The residual amplitude, representing about 20% of the total excitation, stems from the oceans. Rapid polar motion has an irregular nature that is well explained by the combined influence of the atmosphere and the oceans. An overall spectrum reveals cycles principally at 20, 13.6 (fortnightly tidal period) and 10 days (corresponding to the normal atmospheric mode Ψ_3^1), but this is only an averaged feature hiding its strong variability over seasonal time scales. This explains why it is so delicate to determine an empirical model of the tidal effect on polar motion. The variability in both amplitude and phase of the 13.6-day term is probably caused by a lunar barometric effect, modulated by some sub-seasonal thermal processes. The irregularities of the prominent cycles of the short-term polar motion are well explained by the atmospheric and oceanic excitations. The oceanic variability reinforces the atmospheric one, as they were triggered by the same agent, maybe seasonal and inter-annual thermal variations.

Keywords Earth rotation · Rapid polar motion · Atmosphere · Oceans · Excitation · Lunar tide

1 Introduction

The paper is devoted to the short-term wobbles of the rotation pole within the Earth, from 2 to 20 days, designated as rapid polar motion. It is determined from the high-frequency part of the routine daily pole coordinates series, from 0.05 cpd (cycle-per-day) up to the Nyquist frequency 0.5 cpd, and represents less than 1% of the total power spectrum. Its amplitude remains less than about 2 mas (milliarcsecond), as shown in Fig. 1 for the year 2008. However, the 50 μas (microarcsecond) accuracy of pole coordinates, as determined by Global Positioning System (GPS), and to a lesser extent Satellite Laser Ranging (SLR) and Very Long Baseline Interferometry (VLBI), permits us to investigate those tiny oscillations in light of the geophysical excitation that causes them. The atmosphere and oceans are known to be the major contributors in this frequency band. The present modelling of the associated angular momentum allows detection of weekly or bi-weekly variations below 2 mas, such as the loops of the winter 2005–2006, analysed by Lambert et al. (2006). Rapid polar motion was predicted as early as the 1980s from estimates of the atmospheric angular momentum, which clearly exhibited large but irregular variations under 20/30 days, as large as the seasonal one; see the wavelet analysis in Fig. 2. A "7-week" fluctuation was noted by Barnes et al. (1983). By this time the precision of pole coordinates was 2 mas and the corresponding effect in the polar motion could not be detected. Owing to the development of VLBI, rapid polar motion was put forward little by little and related to the atmospheric angular momentum (Eubanks et al. 1986, 1988; Brzeziński 1987; Nastula et al. 1990), and convincingly confirmed after 1990 when polar motion accuracy dropped below 0.2 mas (Gross and Lindqwister 1992; Nastula et al. 1997) with the advent of the GPS technique. With progress in global ocean circulation models, the role of the ocean was demonstrated around 2000 (Nastula and Ponte 1999; Ponte and Ali 2002). After an extensive comparison of the best pole coordinate series with atmospheric and oceanic angular momenta for data prior

C. Bizouard (✉) · L. Seoane
Paris Observatory, SYRTE, Paris, France
e-mail: christian.bizouard@obspm.fr

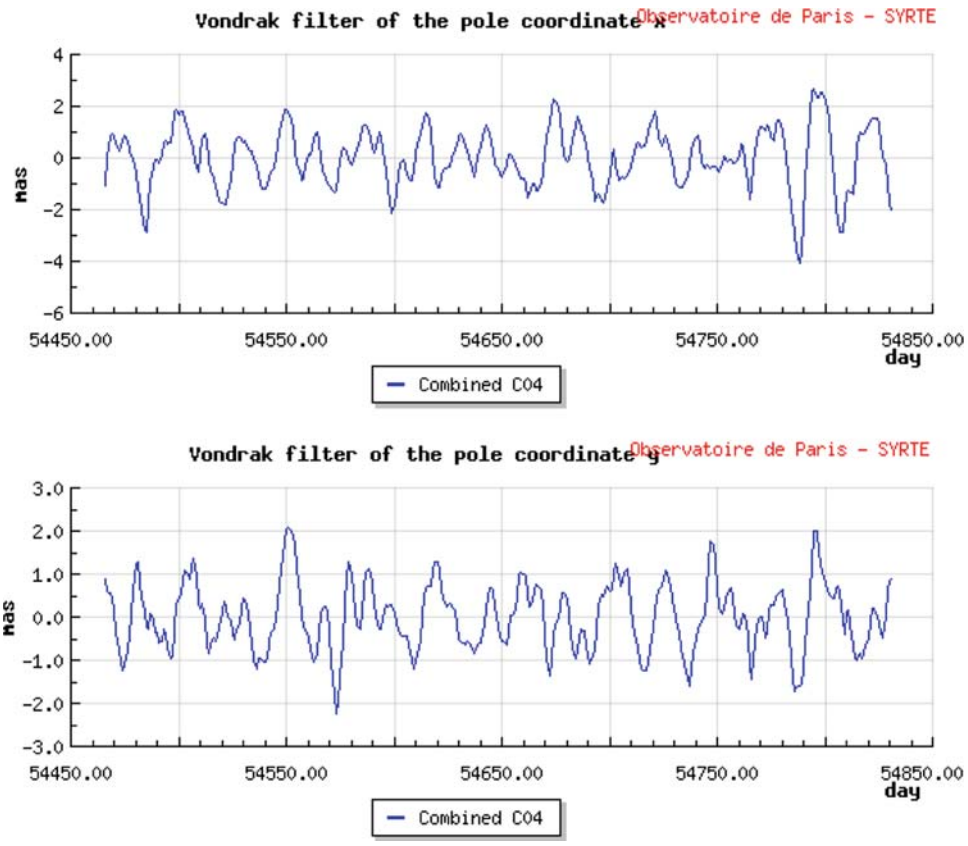

Fig. 1 A Vondrak filter applied to the pole coordinates x and y (C04 series) over the year 2008 (MJD 54466–54831) to isolate the fluctuations below 20 days, called the rapid polar motion. Almost bi-weekly variations are conspicuous. Plot extracted from the web site of the IERS Earth Orientation Centre (http://hpiers.obspm.fr/eop-pc). See Sect. 2 for filter parameters

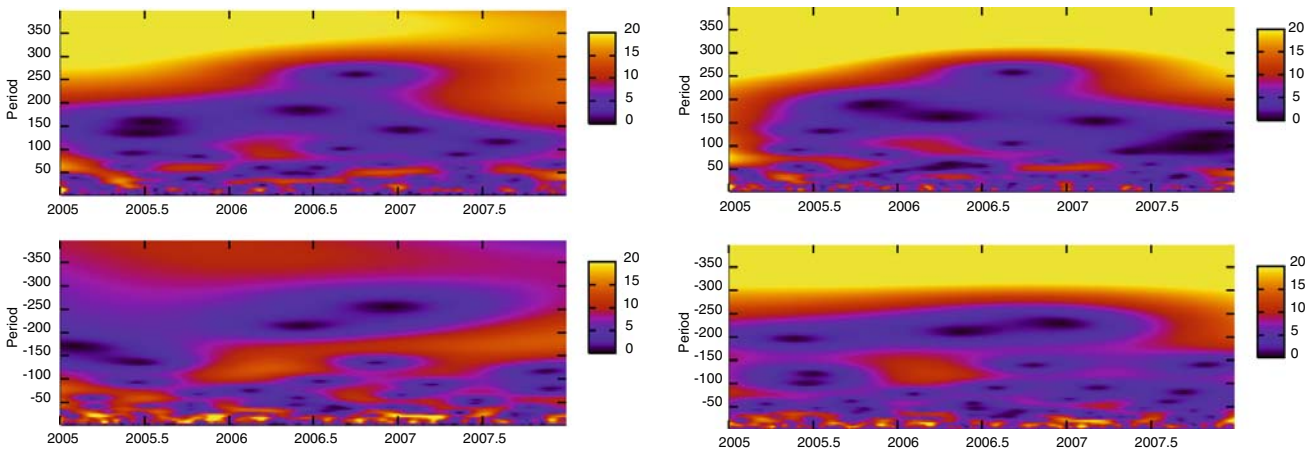

(G) (AO)

Fig. 2 Morley wavelet analysis of geodetic excitation (G, *left panel*) and Atmospheric/Oceanic excitation (AO, *right panel*) between 5 and 400 days from 2005 to 2008. Amplitude in mas. Two frequency bands take shape and dominate the equatorial excitation: the regular prograde seasonal band (*top row*) and the episodic retrograde excitation (*bottom row*) below 20 days. See Sect. 2 for data description

to 2000, Kouba (2005) concluded that the atmosphere and oceans can explain many features of the polar motion, down to 2.5 days, with a drop of correlation for periods below 5 days. More recent studies are lacking, so we thought it valuable to revisit short-term polar motion excitation using the most recent geodetic, atmospheric and oceanic data. The following points deserve particular attention.

Below 10 days, the oceans do not react exactly like an inverted barometer in response to atmospheric pressure variations (see e.g. Salstein and Rosen 1989). The data

assimilation and circulation model for atmosphere and oceans needs to be tested for frequencies approaching diurnal, for which atmospheric and oceanic angular momenta are poorly estimated. On the other hand, polar oscillation measurements are degraded for periods close to 2 days, the Nyquist period of daily pole coordinates series estimated in routine analysis of GPS, VLBI and SLR observations. We are interested to know to what extent the combined influence of the atmosphere and oceans reproduce the geodetic excitation for that frequency band.

Irregular behaviour, well illustrated by the appearance of loops, is a key feature of rapid polar motion. Therefore, the harmonic nature of some spectral peaks has to be questioned: what about the influence of the oceanic tides, recently revisited by Gross (2009), at 13.6 days, and the effect of the normal atmospheric mode around 10 days detected by Brzeziński (1987)?

By considering the most recent pole coordinates and atmospheric/oceanic angular momentum series, we hope to answer those questions, and to show the relevance of short-term polar motion for both geophysics and Earth rotation, despite its small amplitude.

2 Data and methodology

Our study is based upon the daily pole coordinates of the combined IERS C04 series (at 0 h UTC) (Bizouard and Gambis 2009). They are mainly based on International GNSS Service (IGS) combined series, with a small contribution of the International VLBI Service (IVS) combined series. Because the sampling at 0hUTC and smoothing perturb the high-frequency components ([0.2, 0.5] cpd) of daily pole coordinate series such as C04 or IGS (Kouba 2005), we also include in our analysis the "ultra-rapid" IGS series, labeled IGU (subsampled at 0 and 12 h UTC) to investigate that frequency range. The time interval under consideration is the period 2005–2009, from which we can draw the general features of the short-term polar motion. This time interval can indeed be considered as representative, at least since 1998 when the mean precision of the pole coordinates became less than 0.1 mas, and we have checked that analysing other time intervals does not change the nature of our results.

These series are matched over the same period with: Atmospheric Angular Momentum (AAM) of the National Centre for Environmental Prospect/National Centre for Atmospheric Research (NCEP/NCAR) reanalysis model, sampled at 0, 6, 12, 18 h UTC, provided by the Sub-bureau for Atmosphere of the Global Geophysical Fluid Centre (GGFC) (SBA 2009); Oceanic Angular Momentum (OAM) of the ECCO model kf066b (MIT), with assimilation of altimeter measurements, compatible with NCEP Inverted Barometer AAM, sampled at 0 h, provided by the Sub-bureau for Oceans of the GGFC (SBO 2009). As usual, angular momentum is split into the matter term (superscripted "mat")—associated with inertia moment of the layer, reflecting the mass distribution—and the motion term (superscripted "mot")—the relative angular momentum stemming from the mass displacements with respect to the crust (Barnes et al. 1983). As the matter term is obtained by integrating a surface pressure function, it is also called the pressure term or bottom pressure term in the case of the oceans. The motion term is naturally called wind term for the atmosphere and current term for the oceans. Those angular momenta are commonly reduced to non-dimensional quantities, called effective angular momentum function, hereafter denoted as χ^{eff} for their complex equatorial part. Then, the linearised Euler–Liouville equation ruling the polar motion in the case of an anelastic Earth model takes the simple form (Barnes et al. 1983; Brzeziński 1994):

$$p + i\frac{\dot{p}}{\sigma_c^*} = \chi^{\mathrm{mateff}} + \chi^{\mathrm{moteff}} = \chi^{\mathrm{eff}} \tag{1}$$

Here, $\sigma_c = 2\pi/433$ rad/d $+i\alpha$ is the complex Chandler frequency accounting for damping α. This equation holds for routine polar motion: outside the retrograde diurnal band, it is not modified by the secondary resonance caused by the Free Core Nutation. Moreover, for periods below 20 days, far from the Chandler resonance, the effect of damping α is negligible. In the frequency domain we have the equation:

$$p(\sigma) = \frac{\sigma_c}{\sigma_c - \sigma}\chi^{\mathrm{eff}}(\sigma) = T(\sigma)\chi^{\mathrm{eff}}(\sigma) \tag{2}$$

where the "geophysical transfer function" $T(\sigma)$ is exhibited. Having obtained $\chi^{\mathrm{mateff}}(\sigma)$ and $\chi^{\mathrm{moteff}}(\sigma)$ for the atmosphere and the oceans by direct Fourier transform with Hanning windows, the corresponding amplitude $p(\sigma)$ of the polar motion is computed by applying Eq. (2). The frequency resolution is about $1/(4 \times 365) \approx 0.0007$ cpd.

In a second approach, the geodetic excitation function given by:

$$\chi_G = p + i\frac{\dot{p}}{\sigma_c} \tag{3}$$

is compared to the atmospheric and oceanic equatorial excitation functions. The geodetic function is computed using the digital filter proposed by Wilson (1985):

$$\chi_t^G = \frac{i}{\sigma_c 2h}\mathrm{e}^{-i\sigma_c h}(p_{t+h} - p_{t-h}\mathrm{e}^{2i\sigma_c h}) \tag{4}$$

where h is the time step.

The pressure term of the AAM series is the one computed according to Inverted Barometer (IB) response of the oceans, whereas the ECCO OAM series integrates the non-equilibrium processes, not included in "IB oceans", and forced by the winds of the NCEP model.

Before performing the analysis, to avoid contamination of the spectrum by the seasonal and diurnal peaks, we remove the long periodic part of the signal and its diurnal component by applying a Vondrak filter (admittance larger than 99% for periods between 2 and 20 days, admittance lower than 5% for periods above 70 days and below 0.6 day) to the Earth Orientation Parameters (EOP) as well as to the angular momentum of the fluid layers (Vondrak 1969, 1977).

3 Spectral comparison

3.1 Polar motion in the range of 5–20 days (0.05–0.2 cpd)

The frequency band [0.05, 0.2] cpd is well determined by routine analysis of GPS, and to a lesser extent SLR and VLBI observations. Daily time series of pole motion resulting mostly from GPS observations, such as the combined solutions C04, IGS, IERS Bulletin A, SPACE (that can be inter-compared on http://hpiers.obspm.fr/eop-pc) do not present significant difference in that frequency band, and the C04 series is chosen as a good representative of the pole coordinates to perform our analysis. The spectrum of the C04 solution is displayed in Fig. 3 together with the associated contributions of the atmosphere (A), the oceans (O), and their combined effect (AO). Together with those spectra are included the separated contributions of the matter (atmospheric/oceanic bottom pressure) and motion terms (wind/current).

Between 5 and 20 days, the spectral agreement between AO influence and observed polar motion is very satisfactory. There is globally more power in the retrograde band than in the prograde one. This is probably associated with the normal atmospheric mode around 10 days, a westward pressure wave denoted Ψ_3^1 by meteorologists and detected in AAM and polar motion by Brzeziński (1987), confirmed by Brzeziński et al. (2002), and appearing in Fig. 3 at the level of 150 μas. Its frequency is not precisely localised and extends over the range $[-0.10, -0.12]$ cpd. It is accompanied by a broadband prograde peak exceeding 100 μas. The most prominent peaks (250 μas) at ± 0.05 cpd, that is the normal mode half-frequency, can also be attributed to this normal mode strongly reinforced by the oceanic influence. It has to be noted that the relative symmetry between prograde and retrograde band is caused by the inverted barometer behaviour of the oceans in the face of atmospheric pressure change. For the non-inverted barometer AAM, the retrograde band is much more powerful than the prograde one and the retrograde nature of the Ψ_3^1 mode is emphasised.

In order to assess the level of significance of these spectral peaks, we assume that the noise of pole coordinate series is represented by the time series differences of the individual or combined GPS series (C04 included). We note that the Allan variance of these offsets $\sigma_a^2(\tau)$ (Allan 1987; see also Allan's web site http://www.allanstime.com) is always a flat function of the sampling interval τ, characterising a flicker frequency noise of maximal variance $\sigma_a^2 = 10^4\ \mu\text{as}^2$ in the worst case. At a given frequency f this noise has the spectral power density $\frac{\sigma_a^2}{2\ln(2)f}$ where f is the frequency. The corresponding spectral amplitude is:

$$\sigma(f) = \sqrt{\frac{\sigma_a^2}{2\ln 2 f T}} \tag{5}$$

where T is the time interval for computing the spectrum. With $T = 4$ years, we obtain $\varepsilon(f) = 2.2 f^{-0.5}$ μas for f in cpd. This flicker frequency noise decreases from about 10 μas at 0.05 cpd to about 5 μas for 0.2 cpd. According to this noise estimate, the previous spectral peaks attain at least the 7σ confidence level, and the averaged spectral power apart from the peaks, reflecting the non-harmonic feature of the rapid polar motion, is above the estimated spectral noise.

Besides 10 and 20 days oscillations, peaks at ± 0.073 cpd (13.6 days), corresponding to the frequency of the fortnightly tide, are noticeable with an amplitude larger than 150 μas (15σ), with a clear lack of power in geophysical fluid excitation (AO). Instead of incriminating the quality of the geophysical models, the peaks probably reflect the most important tidal effect on polar motion, precisely at 13.6 days and amounting to typically 50 μas according to the Dickman model (1993) reported by Gross et al. (1998) in term of tidal harmonics in equatorial excitation function (≈ 1.7 mas for -13.66 days). This assumption is checked by adding back the improved empirical model of Gross (2009) to the combined fluid excitation (AO) and re-estimating the polar motion effect. The total fluid effect (AOT), including the tidal effect (T), shows much smaller discrepancy with respect to observations at the prograde fortnightly frequency (Fig. 3). This emphasises the Mf(13.66 days)/mf(13.63 days) oceanic tidal effect in polar motion, as detected by Gross et al. (1998) after removing geophysical excitation reduced to IB AAM. According to Fig. 3, the non-tidal oceanic signal, as large as the atmospheric one, has to be removed as well from the observed polar motion to isolate the pure invariable tidal effect, as done recently by Gross (2009) also using the NCEP/ECCO model.

The above-mentioned studies also report a tidal effect at 9.1 days (0.11 cpd) (less than 10 μas), that very slightly perturbs the polar motion amplitude at 0.11 cpd (Fig. 3), and does not explain the geodetic power found at that frequency. According to the spectrum in Fig. 3, it is mostly caused by the atmosphere in association with the free mode Ψ_3^1.

By the way, the 13.6-day (0.073 cpd) and 9.1-day (0.11 cpd) oscillations contain a large atmospheric signal and a non-tidal oceanic signal to a lesser extent. According to Kouba (2005) that extra-tidal 13.6 days term is an artefact,

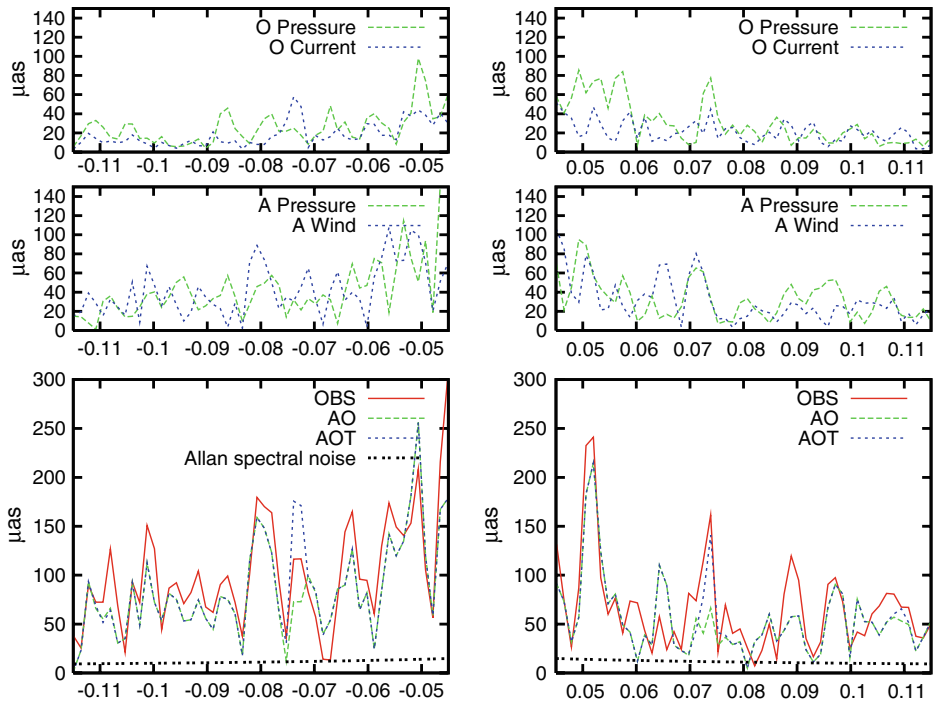

(a) from 0.05 to 0.11 cpd - amplitude range : 300 μas.

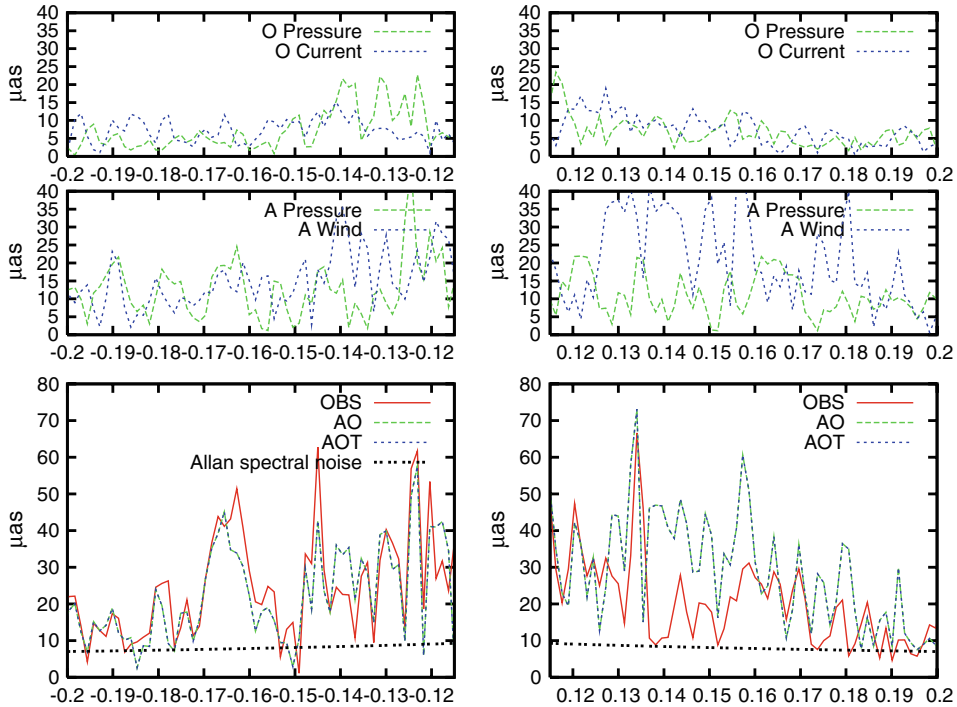

(b) from 0.11 to 0.2 cpd - amplitude range : 80 μas.

Fig. 3 Complex spectrum (retrograde left panels, prograde *right panels*) of C04 pole coordinates $x - iy$ (*OBS*) compared to corresponding contributions of the atmosphere (*A*), oceans (*O*), both fluid layers (*AO*) including ocean-tide effects (*AOT*) in the frequency band [0.05, 0.11] cpd (**a**) and [0.11, 0.2] cpd (**b**). Period 2005–2009. Note the peaks at ± 0.05 cpd (20 days), ± 0.073 cpd (13.6 days), broad band peak at ± 0.1 cpd (10 days, associated with the atmospheric normal mode Ψ_3^1) and the dominant retrograde band. All these peaks are well above the estimated spectral noise

associated with GPS processing, not observed in VLBI polar motion, at least before the year 2000. But, our own analysis, based upon the most recent VLBI and GPS series received at the IERS Earth Orientation Centre, shows that VLBI data also contain that term. So it deserves study as a geophysical fluctuation. As no thermal source is known at that period, the most probable cause is the lunar fortnightly tide. Such a tidal atmospheric forcing is not well documented. It has been observed in both surface pressure (Arabelos et al. 1997, 2004) and zonal winds (Li 2005). According to the measurements of Arabelos et al. (2004) in the area of Thessaloniki, that tidal pressure oscillation is up to 25 Pa, about a quarter of the diurnal fluctuation, and causing a prograde diurnal polar motion up to 10 µas (Brzeziński et al. 2002). The transfer function

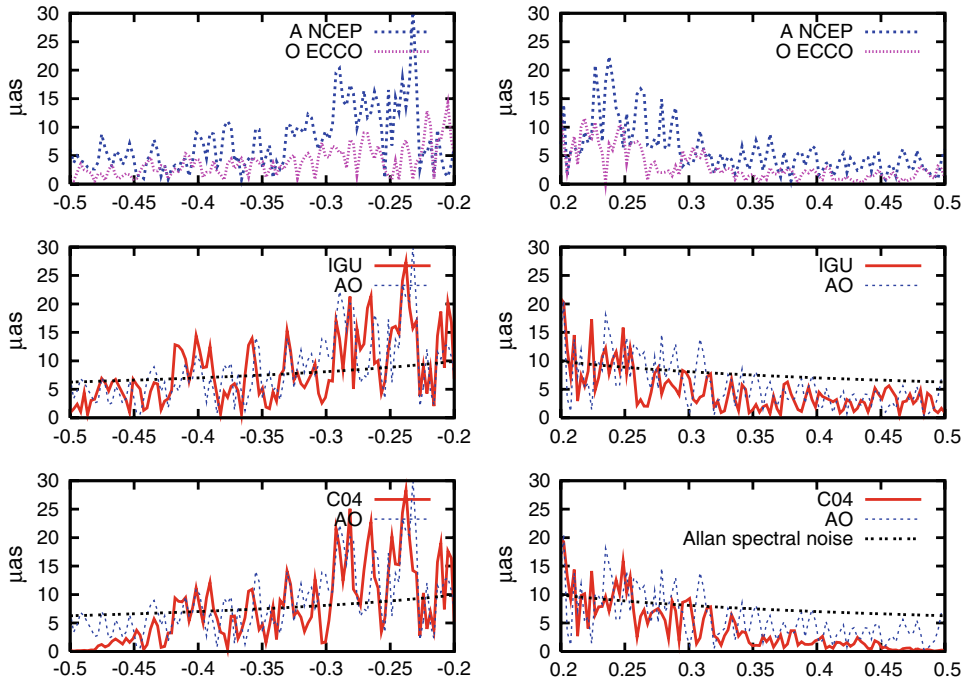

Fig. 4 Complex spectra of daily C04 and IGS Ultra rapid (*IGU*) pole coordinates $x - iy$ with corresponding contributions of the atmosphere (*A*), oceans (*O*), both fluid layers (*AO*) in the frequency band [0.2, 0.5] cpd ([2,5] days). Symmetric peaks arise at about 0.21, 0.24 cpd. The spectra are restricted to the period 2007–2009 to avoid the broadening of the peaks caused by the strong irregularities of the fluid layer in that frequency band (see Sects. 4, 5)

$T(\sigma)$ (Eq. 2) is about ten times more powerful at ± 0.073 than at $+1$ cpd for the matter term. So if the order of the Mf barometric tide of Thessaloniki is true on a planetary scale, we predict that the lunar barometric effect can reach the value $10 \times 10/4 = 25\,\mu$as, which is overwhelmingly observed in the atmospheric pressure term. The complex response of the atmosphere to the lunar tide would also explain the presence of the second harmonic at 0.145 cpd (Fig. 3) and the double peak at 0.21–0.22 cpd close to the third harmonic (Fig. 4).

Moreover, this spectrum allows us to assess the accuracy of the combined atmospheric/oceanic angular excitation from the spectral offsets AOT–OBS, as far as other geophysical effect are supposed to be negligible: about $|\mathrm{AOT}-\mathrm{OBS}|/|T(\sigma)|$ where T is the transfer function defined by Eq. (2). For instance for the biggest offset at -0.1 cpd we obtain $40\,\mu\text{as}\ 2.3 \approx 20\,\mu$as. Any offsets $|\mathrm{AOT} - \mathrm{OBS}|$ in the spectral band, above the spectral noise of the pole coordinates, can be mainly attributed to the defects in AAM and OAM.

3.2 Polar motion in the range of 2–5 days (0.2–0.5 cpd)

According to the spectra in Fig. 4, pole coordinates exhibit almost symmetric peaks at about 0.21 cpd, 0.24/0.25 cpd with a power below $20\,\mu$as. Again we notice more power in the retrograde band. Because of its daily intervals, the C04 spectrum is attenuated for frequencies approaching 0.5 cpd, and for frequencies larger than 0.3 cpd shows less power than the fluid forcing. The majority of daily pole coordinate series, such as the C04 or IGS combined solutions present such a damping. Such a defect is not present in the four daily Ultra rapid IGS series, labelled IGU, subsampled at 0 and 12 h UTC (for minimising diurnal variation). The IGU spectrum in the range [0.2,0.5] cpd is confirmed by a GRGS multi-technique combination (Gambis et al. 2009) performed at Paris Observatory over the year 2007–2008. Meanwhile SLR daily series of the Centro di Geodezia Spatiale (CGS) and International Laser Ranging Service (ILRS) also present required power in the range [0.2, 0.5] cpd, but with significant discrepancies with respect to GRGS and IGU series. As GPS is known to be more reliable for pole coordinates than SLR, we discarded those SLR series for the geophysical analysis. Power is also present at -0.29 cpd, curiously the fourth harmonic of the fortnightly frequency, coming after 0.145 cpd (second harmonic) and 0.22 cpd (third harmonic), and mostly originating in the atmosphere. With an amplitude larger than $5\,\mu$as are noticeable supplementary peaks at $-0.34/-0.4$ cpd, mostly of atmospheric origin. However, these latter peaks are hardly greater than the noise, as estimated by Allan variance.

4 Excitation and its time variability

The excitation function is a dimensionless measure of angular momentum at work, in some way related to the energy of the angular momentum variations. Both geodetic (*G*) and *A*/AO excitation are first compared in the time domain. We compute corresponding correlations, reported in Table 1, as well as the part of the variance of geodetic variations (*G*) explained by the atmospheric (*A*) or atmospheric–oceanic (AO) components—the fractional variance explained

Table 1 Correlation between geodetic (G, C04 series) and A/AO excitation and percentage of the variance of G explained by A/AO excitation

Band	Correlation		Explained variance (%)	
	x	y	x	y
2–5 days				
$G-$AO	0.74	0.75	42	39
$G-A$	0.66	0.65	36	26
5–20 days				
G/AO	0.91	0.91	81	83
G/A	0.81	0.80	64	63
20–50 days				
G/AO	0.86	0.92	74	83
G/A	0.70	0.73	48	52

The computations are done over 2005–2008. The results for IGU series do not differ significantly

being defined by $[\mathrm{var}(G) - \mathrm{var}(G - \mathrm{AO})]/\mathrm{var}(G)$. These computations are done for three frequency bands, grossly split by Vondrak filtering: [2,5] days, [5,20] days, [20,50] days (at the edge of those bands admittance is 95%, except for 2 days where admittance drops to 80% for removing the diurnal atmospheric effect). In all the cases, the oceans contribute positively. Moreover, not shown here, the matter term does not exceed the motion term by much, as in the case of the seasonal band.

For oscillations below 5 days, agreement between geodetic (G) and atmospheric (A) variations or G/AO variations deteriorates. Correlations of 90% in the band [5,20] days drop to 75% in the band [2,5] days. The AO forcing explains 80% of the geodetic variance above 5 days, but less than 50% below 5 days. Although the IGU series better account for the spectral amplitude of the AO contribution for spectral peaks close to 2 days (see Sects. 3, 5), the C04 and IGU geodetic excitation are globally as well correlated to the AO excitation in the band [2,5] days.

The band [5,20] days exhibits even stronger match between pole coordinates and atmospheric/oceanic forcing than for the band [20,50] days, where possible hydrological processes may perturb the budget, as in the case of the seasonal band.

The Fourier spectra of the former section do not tell anything about possible variability of the excitation. From the Morley wavelet transform, displayed in Fig. 5 (over the reduced interval 2005–2008 for a better graphical representation), the geodetic excitation (G) presents amplitudes up to 30 mas on sub-seasonal scales. The small rapid polar motion is associated with an atmospheric/oceanic angular momentum exchange sometimes larger than at seasonal periods (15 mas), but clearly irregular, as shown in Fig. 5. On the same figure, we see how well the combined AO excitation assumes the form of the geodetic excitation, with a lack of power noticeable in the retrograde band, as if AO excitation had been underestimated. For prograde components, the 13–14 days oscillation is dominant and often excited in concordance with the 10 and 20 days harmonics. Retrograde excitation reaches slightly larger amplitude and is dominated by the atmospheric normal mode at 10 days and the half-frequency mode.

Below 5 days, that excitation remains important, up to 10 mas. The retrograde band around 3–4 days (-0.3 cpd) stands out in the wavelet analysis in Fig. 6, in both the AO excitation and geodetic excitation, especially when taking the IGU pole coordinates. As expected from correlation analysis, the patterns drawn by the fluid layer excitation do not fit the observed ones as well as in the band 5–20 days.

5 Time variability at given frequencies

5.1 Irregularity of the short-term cycle determined by sliding window fit

The variability at some frequency can be better determined by fitting the corresponding cycles over sliding windows of 0.3 year. The corresponding frequency resolution of about 0.01 cpd is sufficient to distinguish the terms at frequencies $f_k = 0.05, 0.07, 0.10, 0.14, 0.21, 0.24, 0.29, 0.34$ cpd. For polar motion $p = x - iy$, A and AO contribution, we fit the cosine term a_k and sine term b_k or equivalently the amplitude A_k and phase Φ_k such as:

$$p = \sum_k a_k \cos(2\pi f_k(t - t_0)) + b_k \cos(2\pi f_k(t - t_0)) = \sum_k A_k e^{i(2\pi f_k(t-t_0)+\Phi_k)} \quad (6)$$

where t_0 is the epoch 2000. Then, we compute the complex correlation coefficients between the signals $A_k^{\mathrm{OBS}}(t)e^{i\Phi_k^{\mathrm{OBS}}(t)}$ and $A_k^{A/\mathrm{AO}}(t)e^{i\Phi_k^{A/\mathrm{AO}}(t)}$ and the percentage of variance explained by the AO variability. For each prominent peak the results over 2005–2008 are reported in Table 2. They globally show very good agreement between OBS and AO contribution, with correlations up to 90% over 2005–2008. The decreasing correlation and explained variance with increasing frequency is another expected feature. Whereas above 5 days C04 and IGU pole series give the same results, for cycles below 4 days (frequencies from 0.25 cpd), IGU matches better the AO forcing (as seen in Sect. 3), and results are distinguished.

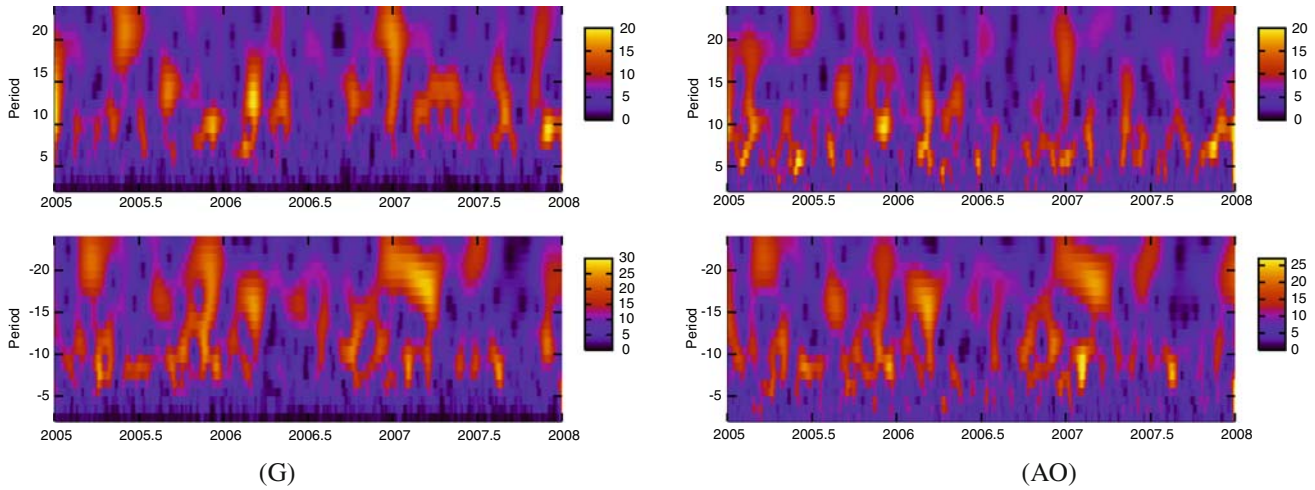

Fig. 5 Morley wavelet analysis of geodetic excitation (*G*, *left panel*) and atmospheric/oceanic excitation (*AO*, *right panel*) between 5 and 20 days from 2005 to 2008. Amplitude in mas. Fluid excitation well reproduces the irregular patterns of the observed excitation, with slightly less power in the retrograde band (*lower row*) compared to the prograde bands (*top row*)

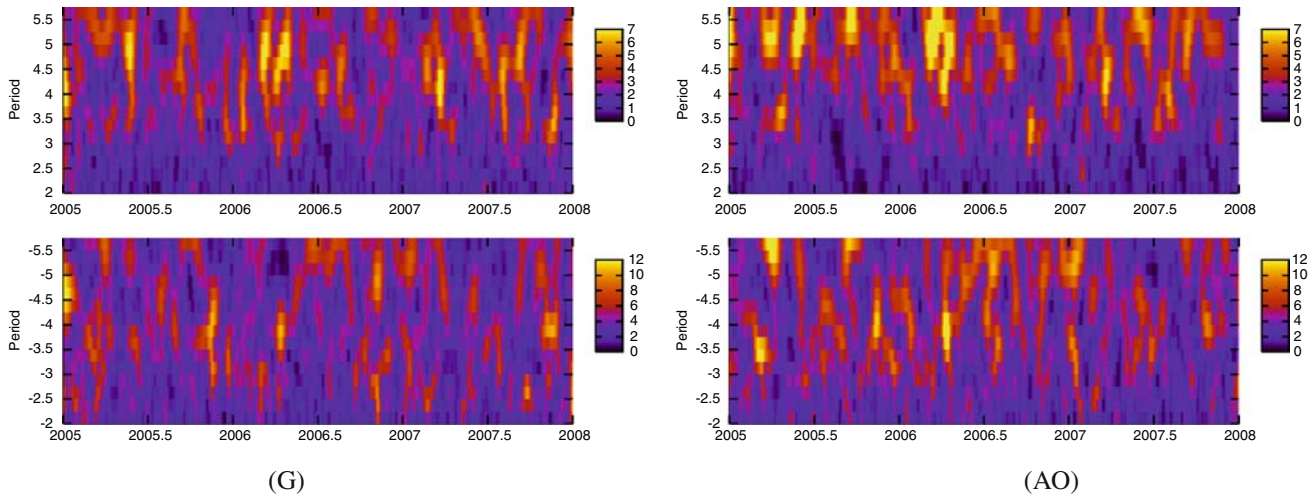

Fig. 6 Morley wavelet analysis of the Geodetic excitation (*G*, *left panel*) and atmospheric/oceanic excitation (*AO*, *right panel*) between 2 and 5 days from 2005 to 2008. Amplitude in mas. Here, geodetic excitation is derived from the IGU pole coordinates series; using the C04 series the power of the band around 3–4 days is reduced

5.2 Time variability at tidal frequencies

In Fig. 7 are shown both observed variation and those estimated from *A* and AO excitations for 13.6 days; also superimposed are the associated correlations as well the explained variance of the observed excitation. Very striking are variations as large as their mean values and very well correlated, up to 90% over 2005–2008 for the prograde cycle, as if the barometric peaks Mf/mf are strongly modulated by a process that is still to be investigated. Though irregularity is mainly caused by the atmosphere, oceanic enhancement is noticeable. According to Table 2, a similar conclusion can be drawn for the second harmonic at 0.14 cpd.

The sub-seasonal modulation of the 0.073 cpd cycle has the same level as the tidal effect (100 μas), and explains the difficulty to determine exactly fortnightly tidal constituent in polar motion and build an empirical model of the effects of the long-period ocean tides on polar motion. However, if that oscillation is fitted over many years after removal of AO excitation, residual variability is averaged, and remains the pure tidal effect. Therefore, by increasing the time interval of fit, Gross (2009) has noticed a convergence of the amplitude and phase of the tidal harmonics mf

Table 2 Complex correlation $re^{i\Phi}$ between variable harmonics of the rapid polar motion (OBS) and the atmospheric/oceanic contribution (A/AO), variance of the observed variability and explained percentage

Frequency (cpd)	Correlation				Variance	Explained variance (%)	
	OBS/A		OBS/AO		OBS	OBS/A	OBS/AO
	r	$\Phi(^\circ)$	r	$\Phi(^\circ)$	μas^2		
−0.05	0.86	−2	0.97	−8	73^2	71	90
+0.05	0.78	−0	0.89	11	94^2	61	76
−0.07	0.86	−1	0.94	−1	37^2	68	84
+0.07	0.74	23	0.86	8	73^2	45	71
−0.10	0.92	−6	0.95	10	20^2	77	84
+0.10	0.80	7	0.85	6	24^2	58	71
−0.14	0.85	−9	0.92	12	99^2	64	77
+0.14	0.78	0	0.77	9	69^2	57	57
C04							
−0.21	0.48	2	0.67	−8	35^2	22	44
+0.21	0.61	10	0.70	−7	28^2	37	48
−0.24	0.47	36	0.68	27	36^2	−2	28
+0.24	0.40	51	0.57	29	28^2	−23	5
−0.29	0.72	−3	0.74	2	26^2	51	54
−0.34	0.37	18	0.42	14	14^2	1	3
IGU							
−0.21	0.48	4	0.67	−8	34^2	22	43
+0.21	0.59	12	0.68	−7	28^2	33	45
−0.24	0.45	32	0.68	23	35^2	−3	31
+0.24	0.40	42	0.59	23	27^2	−18	10
−0.29	0.76	13	0.76	−7	25^2	54	55
−0.34	0.52	−6	0.58	−2	15^2	26	31

Above 5 days, EOP series C04 and IGU give the same results, but for frequencies approaching 0.5 cpd, IGU series better matches AO effect than C04, and results are distinguished. The computation is done over 2005–2008. Note the decreasing correlation and explained variance with increasing frequency

(13.63 days) and Mf (13.66 days) over intervals longer than 10 years.

5.3 Time variability at 0.05 and 0.1 cpd

As for the averaged spectral power, the variability of the 10 days mode, shown in Fig. 7, is dominated by the atmosphere with 90% correlation level. The retrograde frequencies −0.05 and −0.01 cpd are those for which the AO variability matches the best the geodetic one. The role of the oceans is minor at 10 days, but it is clearly conspicuous in the half frequency mode in 20 days.

5.4 Time variability above 0.2 cpd (below 5 days)

The irregularity estimated in observed cycles (OBS) and fluid effects (AO), smaller than 50 μas, present correlations up to 70% in the retrograde band, whereas there is reduced agreement in the prograde band. In any case, the role of the oceans is evident and IGU better accounts for AO irregularities than CO4 for frequencies 0.29/0.34 cpd, as expected.

6 Discussion and conclusion

The rapid polar motion is dominated by three cycles: 20, 10 and 13.6 days (Mf or mf tides), accompanied by secondary oscillation at 6.8 days. Those cycles appear harmonic on the long run, over a few years. Actually at sub-seasonal time scales, the variability in amplitude can reach the same level as the mean spectral power. It is worth noting that the atmospheric and ocean circulation models reproduce not only the mean amplitude and phase of those cycles, but also their variability, despite a slightly smaller power. This underlines the high quality of those models, at least above 5 days. In

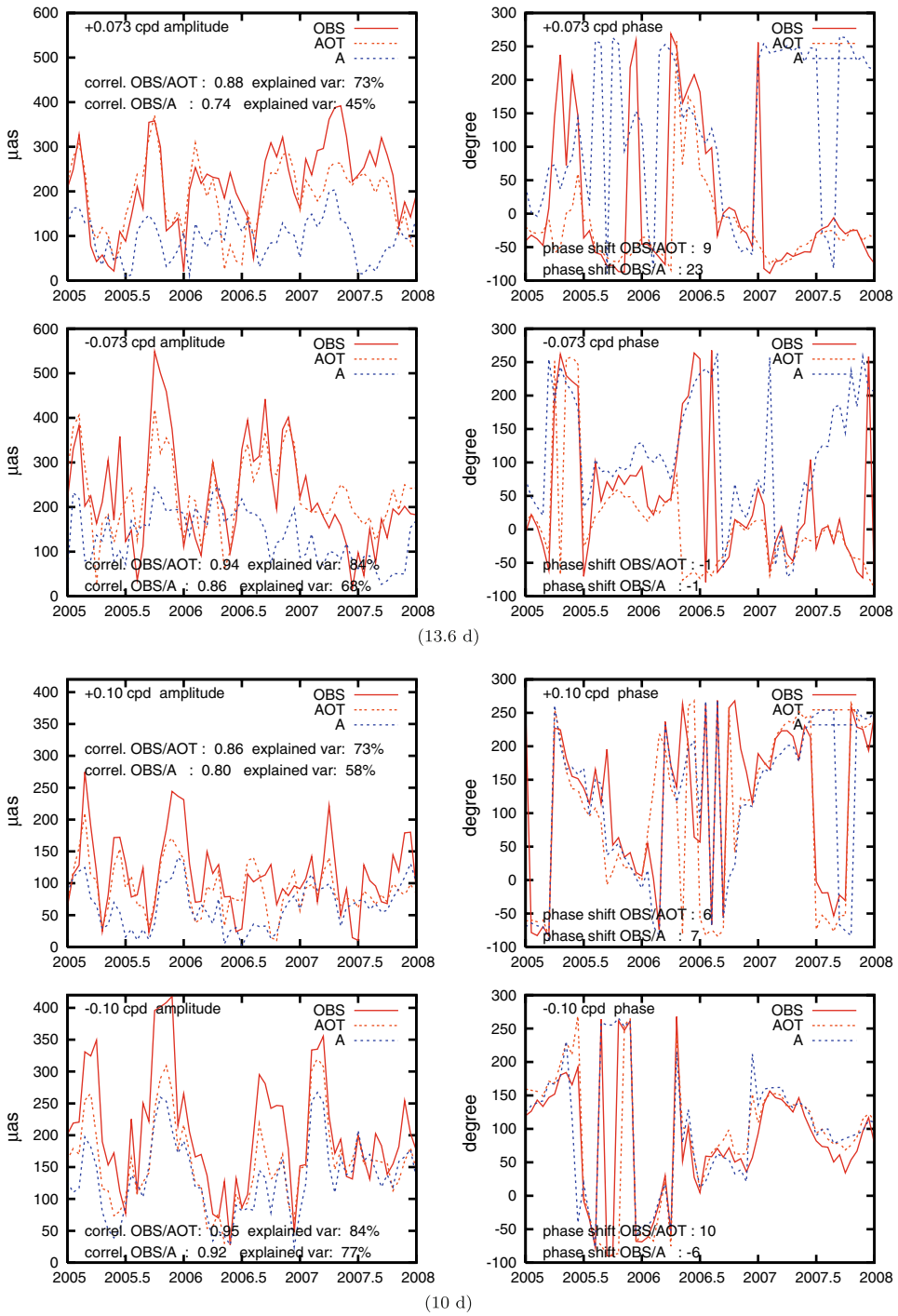

Fig. 7 Estimates of the amplitude (*left panels*) and phase (*right panels*) of the ± 0.073 and ± 0.1 cpd oscillations in geodetic excitation (*OBS*), atmospheric (A), and combined atmospheric–oceanic excitation including harmonic tidal effects (*AOT*) from 2005 to 2008 by least squares sliding window (0.3 year). Visually the AO contribution explains very well the pattern of observed variability at those frequencies, as confirmed by correlation coefficients and percentage of explained variances $[\mathrm{var}(\mathrm{OBS}) - \mathrm{var}(\mathrm{OBS} - A/O)]/\mathrm{var}(\mathrm{OBS})$. At 0.073 cpd, atmosphere and oceans induce concomitant variability of about 200 µas, larger than the tidal oceanic effect. Because of the free mode Ψ_3^1, atmosphere controls the variability at 0.1 cpd

particular, the normal atmospheric mode at 10 days causes an oscillation with an amplitude varying from 50 to 400 µas over 1 year. The combined effect of the atmosphere and non-tidal oceanic angular momentum also produces a very strong variability of the 13.6 days (0.073 cpd) harmonics and its sub-harmonic at 6.8 days (0.145 cpd). This also explains why an invariable tidal effect at 13.6 days is hard to estimate empirically. The presence of power from the atmosphere at the tidal frequencies of 0.073 cpd, 0.11 cpd and their second harmonics suggests that the atmosphere is strongly influenced by the lunar tide, in a way that has to be clarified by future studies. This view is supported by the existence of another lunar tidal constituent in equatorial AAM: the O1 diurnal term reported by Petrov (1998) and later in a review by Brzeziński et al. (2002).

Salstein and Rosen (1989) already noticed that the 10–20 days atmospheric oscillations in AAM mostly result from barometric processes located over oceanic regions,

and concluded that the oceanic response is fundamental for understanding rapid polar motion, a result strengthened by our study. Looking more carefully at Fig. 7 and Table 2, it appears that the oceans reinforce the variations seen in the atmospheric effect, not only at the fortnightly period, as if both fluid layers were influenced contemporaneously by the same agent. Although the variations could to be considered a priori as hazardous, they exhibit more or less seasonal, sub-seasonal or inter-annual patterns, as confirmed by Fourier analysis over 2000–2009 (not shown here). This points out seasonal or slower climatic processes modulating normal and tidal modes, which need to be investigated in the future. It may be a thermal effect at seasonal, semi-annual, inter-annual (El-Nino) time scales, as suggested by the repetitive pattern in the variability of the spectral components.

Our study also stresses significant forcing in the band 3–4 days, up to 10 μas. But below 5 days, pole variations under 10 μas become inaccurate, near the spectral noise level estimated by Allan variance, while the routine daily series are damped for periods approaching the Nyquist period of 2 days. There begins a blind zone that can be investigated only using sub-daily series, for AAM, OAM and pole coordinates, sampled at least every 12 h. If AAM are routinely determined at 6 h time resolution, that is neither the case of OAM for which sub-daily analyses are lacking nor actually the case of IGU pole coordinates. Indeed they represent 24 h integrations. This means the values reported at 0, 6, 12 and 18 h UTC are highly correlated with each other, and do not have a true 6 h time resolution. Below 5 days AAM and OAM may help to discriminate pole coordinate series, for instance to prefer the IGS combined series based on GPS observations with respect to the multi-technique combined C04, as already noticed by Kouba (2005). But above 5 days, contrary to the opinion expressed in the latter paper, which might be valid for data prior to 2000, the AAM and OAM series cannot furnish a reference for qualifying combined pole coordinate series among themselves, such as C04, IGS, Bulletin A, because the spectral noise of their time series differences is much smaller than the spectral noise of their difference with the modelled atmospheric/oceanic effect.

Inspite of the limitations mentioned, pole coordinates as determined by GPS uncover the fine structure of the rapid polar motion with an unprecedented accuracy, confirm the high-accuracy of the angular momentum series (NCEP/ECCO), and hint of the importance of a lunar barometric tide in the rapid polar motion and weekly climatic processes. This reinforces the work of the Russian meteorologist Sidorenkov (2002, 2003, 2008), who claims that climate is strongly driven by the slow luni-solar tides and therefore can be subject to long-term prediction.

Acknowledgments We are grateful to our colleagues Jim Ray, Daniel Gambis, Sébastien Lambert and to the reviewers for the corrections and suggestions brought in this paper, and Jean-Yves Richard for his advise in using the Allan variance.

References

Allan D (1987) Time and frequency (time-domain) characterisation, estimation, and prediction of precision clocks and oscillators. IEEE Trans Ultrason Ferroelectr Freq Control 34:647–654

Arabelos D, Asteriadis G, Contadakis ME, Spatalas SD, Sachsamanoglou H (1997) Atmospheric tides in the area of Thessaloniki. J Geodyn 23(1):65–75

Arabelos D, Asteriadis G, Bloutsos A, Contadakis ME, Spatalas SD (2004) Atmospheric tides disturbances as earthquake precursory phenomena. Nat Hazards Earth Syst Sci 4:1–7

Barnes RTH, Hide R, White AA, Wilson CA (1983) Atmospheric angular momentum fluctuations, length-of-day changes and polar motion. Proc R Soc Lond A 387:31–73

Bizouard C, Gambis D (2008) The combined solution C04 for Earth orientation parameters, recent improvements. In: Drewes H (ed) Springer Verlag Series on International Association of Geodesy Symposia 134. 330 p, ISBN 978-3-642-00859-7

Brzeziński A (1987) Statistical investigations on atmospheric angular momentum functions and on their effects on polar motion. Manuscr Geodetica 12:268–811

Brzeziński A (1994) Polar motion excitation by variations of the effective angular momentum function, II: Extended model. Manuscr Geodetica 19:157–171

Brzeziński A, Bizouard C, Petrov S (2002) Influence of the atmosphere on Earth rotation: what new can be learnt from the recent atmospheric angular momentum estimates? Surv Geophys 23: 33–69

Dickamn S (1993) Dynamic ocean-tide effects on Earth's rotation. Geophys J Int 112:448–470

Eubanks TM, Steppe JA, Dickey JO (1986) The atmospheric excitation of Earth orientation changes during MERIT. In: Proceedings of the international conference on Earth rotation and the terrestrial reference frame, 1985, Ohio State University, Columbus, pp 469–483

Eubanks TM, Steppe JA, Dickey JO, Rosen RD, Salstein DA (1988) Causes of rapid motions of the Earth's pole. Nature 334:115–119

Gambis D, Biancale R, Carlucci T, Lemoine JM, Marty JC, Bourda G, Charlot P, Loyer S, Lalanne L, Soudarin L (2009) Combination of Earth orientation parameters and terrestrial frame at the observation level. In: Drewes H (ed) Springer Verlag Series on International Association of Geodesy Symposia 134, 330 p, ISBN 978-3-642-00859-7

Gross R, Lindqwister U (1992) Atmospheric excitation of polar motion during the GIG'91 measurement campaign. Geophys Res Lett 19(9):849–852

Gross R, Chao BF, Desai S (1998) Effect of long-period ocean tides on the Earth's polar motion. Prog Oceanogr 40(1-4):385–397

Gross R (2009) An improved empirical model for the effect of the long period ocean-tides on polar motion. J Geod 83:635–644. doi:10.1007/s00190-008-0277-y

IERS Conventions (2003) IERS Technical Note No 32, Ed. DD McCarthy and G Petit, p 125

Kouba J (2005) Comparison of polar motion with oceanic and atmospheric angular momentum time series for 2-day to Chandler periods. J Geod 79(1-3):33–42. doi:10.1007/s00190-005-0440-7

Lambert S, Bizouard C, Dehant V (2006) Rapid variations in polar motion during the 2005–2006 winter season. Geophys Res Lett 33:L13303

Li G (2005) 27.3 day and 13.6 day atmospheric tide and lunar forcing on atmospheric circulation. Adv Atmos Sci 22(3):359–374

Nastula J, Gambis D, Feissel M (1990) Correlated high frequency variations in polar motion and of the length of the day in early 1988. Ann Geophys 8:565–570

Nastula J, Kosek W, Kolaczek B (1997) Analyses of zonal atmospheric excitation functions and their correlation with polar motion excitation functions. Ann Geophys 15(11):1439–1446

Nastula J, Ponte R (1999) Further evidence for oceanic excitation of polar motion. Geophys J Int 139(1):123–130

Petrov S (1998) Modeling excitation of Earth rotation: stochastic and nonlinear approaches. PhD thesis, Space Research Centre of the Polish Academy of Science, Warsaw, Poland

Ponte R, Ali A (2002) Rapid ocean signals in polar motion and length of day. Geophys Res Lett 29(15):6

Salstein D, Rosen R (1989) Regional contributions to the atmospheric excitation of rapid polar motions. J Geophys Res 94(D7):9971–9978

SBA (2009) WEB site of the IERS Special Bureau for the Atmosphere. http://ftp.aer.com/pub/anon_collaborations/sba/

SBO (2009) WEB site of the IERS Special Bureau for the Oceans. http://euler.jpl.nasa.gov/sbo/

Sidorenkov (2002) Fizika nestabil'nostey vrazheniya Zemli (Physics of the instabilities of the Earth's rotation). Fizmatlit, Moscow, 384 p, ISBN 5-9221-0244-3 (in Russian)

Sidorenkov N (2003) Influence of the atmospheric tides on the Earth rotation. Celest Mech Dyn Astron 87(1–2):27–38

Sidorenkov N (2008) Lunno-solnechnie prilivi i atmosferenie protsessi (Luni-solar tides and atmospheric processes, in Russian). Priroda 2:23–31

Vondrak J (1969) A contribution to the problem of smoothing observational data. Bull Astron Inst Czech 20:349

Vondrak J (1977) Problem of smoothing observational data II. Bull Astron Inst Czech 28:84–89

Wilson CR (1985) Discrete polar motion equations. Geophys J R Astron Soc 80(2):551–554